

Performance **Evaluation** and **Life Testing** of the S1'1' -100

Charles E. Garner*, James C. Polk*, Keith M. Goodfellow*, Lewis C. Pless†, and John R. Brophy**
Jet Propulsion Laboratory
California Institute of Technology
Pasadena, Ca 91109

ABSTRACT

A cyclic endurance test of the Russian 1.35 kW Stationary Plasma Thruster (SPT)-100 is described. The endurance test is scheduled for 6,000 on/off cycles and 5,000 hours of operation at an input power to the thruster of 1.35 kW. Cycles are 50 minutes of thruster on-time and 23 minutes of thruster off-time. To date 800 cycles and 647 hours of thruster on-time have been completed. Thruster efficiency decreased, from 49% to 44% as the thruster aged; thruster efficiency increased when an auxiliary magnetic field was applied. Variations in thruster performance from cycle to cycle correlate with changes in floating potential and discharge voltage. Significant variations in thruster performance were observed to occur within a single cycle, beginning approximately with cycle 225; performance increased in cycles where oscillations in current and voltage spontaneously decreased. After 800 cycles the beam current density at the center of the plume decreased to 76% of the current density measured at the start of the life test. The outer insulator thickness decreased to 29% of the original thickness measured at the start of the life test. The endurance test is being performed under a cooperative program between Space Systems/Loral, JPL, and the Ballistic Missile Defense organization (BMDO).

INTRODUCTION

Stationary plasma thrusters (SPT) are gridless ion thrusters that were originally developed in the U.S. in the early 1960's.^{1,3} Although efforts in the U. S. to develop high thrust efficiencies failed, efforts in the former U.S.S.R. were quite successful; the SPT was successfully developed during the 1960's and 1970s by Morozov⁴ and others^{5,6} with a unique combination of specific impulse and efficiency. It has been reported that more than 50 SPT-70 thrusters have flown in space, starting with the Meteor 1 in 1969-1970.^{7,8} In 1991 a team of electric propulsion specialists visited the former U.S.S.R. to experimentally evaluate the performance of a 1.35-kW SPT-100 at the Scientific Research Institute of Thermal Processes in Moscow and at "Fakel" Enterprise in Kaliningrad, Russia.^{9,10} The evaluation indicated that the actual performance of the thruster appears close to the claimed performance of 50% efficiency at a specific impulse of 1600 s.⁹

Studies indicate that for north/south station keeping and Earth orbit raising applications of electric propulsion, the optimum specific impulse is in the range of 1,000-2,000

Sec.¹¹ combination of the flight heritage of the SPT-70 and the availability of thrusters and thruster data, has led to increased interest in these thrusters by Western spacecraft manufacturers for primary and auxiliary propulsion applications.

Loral is presently flight-qualifying 1.35-kW, SPT-100 thrusters for north/south station keeping and Earth orbit raising applications and plans to provide these thrusters on their spacecraft.¹² At Design Bureau "Fakel" a steady-state life test is being performed, and performance, plume and EMI/RF evaluations are being conducted at NASA Lewis Research Center.

A key aspect of the SPT-100 evaluation program is characterization of the long term operating behavior of the thruster. Typical mission applications of interest require operating times of several thousand hours. Potential use of the thruster for north-south station keeping of commercial communication satellites will also require the capability for several thousand on/off cycles. To address these objectives a cyclic endurance test is being performed at JPL under a cooperative program between Space Systems/Loral, JPL (under the JPL Affiliates program) and the BMDO. The endurance test is scheduled for 6,000 on/off cycles and 5,000 hours of operation at an input power of 1.35 kW. This paper describes the preliminary results of this cyclic endurance test through the first 800 cycles.

APPARATUS

The SPT-100 thruster endurance test is being performed in a 3.1-m dia. x 5.1-m stainless steel vacuum chamber equipped with three each, 1.2-m diameter helium cryopumps (Fig. 1). The nominal pumping speed for the three pumps combined is 81,000 liters/s on xenon. When the life test was initiated, the effective pumping speed of this facility on xenon was approximately 50,000 m/s, or 62% of the rated speed. The reduced pump speed is due in part to masking of cryopump No. 3 by a beam target, and to placement of graphite louvers which protect the other two pumps from direct plume impingement. The minimum no-load tank pressure was observed to be 3.6×10^{-8} torr.

* Member of the Technical Staff, Advanced Propulsion Technology Group. Member AIAA,

† Member of the Technical Staff, Electric Power Systems Section.

** Supervisor, Advanced Propulsion Technology Group. Member AIAA.

The thruster is mounted near one end of the vacuum tank, directly facing cryopump No. 3, which is positioned at the other end of the vacuum tank. The discharge chamber surfaces of the SPT thruster consist of insulator materials, and it has been demonstrated that the performance of SPT thrusters can be significantly affected by the deposition of a conducting coating on the insulator. To protect cryopump No. 3 and minimize the amount of material sputtered back to the thruster, the facility was lined in graphite, and a graphite beam target was constructed. The beam target consists of 6.4-mm thick graphite panels arranged in a chevron configuration and placed as shown in Fig. 1. Graphite was selected as the target material because of its low sputter yield at the ion energies expected from the SPT. A photograph of the SPT-100 mounted inside the vacuum chamber is shown in Fig. 2. The chevron configuration results in large angles (typically greater than 90 degrees) between the expected ion trajectories and the direction normal to the graphite surface, which may both reduce the graphite sputter rate and reduce the amount of sputtered material directed back towards the thruster. A water-cooled plate was positioned between the beam target and cryopump No. 3 to reduce heat radiation to the pump.

Due to the beam divergence characteristics of the SPT-100, material can be sputtered from the vacuum tank sidewall and deposited onto the thruster. Therefore the cylindrical side walls of the vacuum chamber were also lined with graphite panels. The graphite beam target panels were baked out at high temperature (approximately 2300 K) prior to installation in order to minimize the potential for hydrocarbon contamination. The side panels, which are subject to a much lower thermal load during thruster operation, were not. Glass slides were placed 21 cm to either side of the SPT thruster such that material back sputtered to the SPT could be quantified and characterized.

Tank pressure was measured using two ion gauges. One gauge tube was mounted directly to the outer wall of vacuum tank; the other tube was mounted inside the vacuum tank, approximately 0.51 m above and 0.58 m behind the SPT-100. This tube was calibrated on xenon and nitrogen using a spinning rotor gauge that is traceable to NIST; data from this calibration were used to generate a curve fit that was used to calculate tank pressure.

The propellant system for supplying xenon to the SPT-100 thruster is shown in Fig. 3. The system was constructed from 0.64-cm-dia stainless-steel tubing that was scrubbed with acetone and alcohol before assembly. Prior to operating the SPT, the propellant system was checked for dew point, hydrocarbon contamination, and particulate contamination, from valve HV-5 (Fig. 3) to the SPT propellant feedline connector. Checks were performed by flowing 4389 cm³ of nitrogen into the instrumentation; results for particulate contamination are shown in Table 1.

Table 1. Particulate Contamination in the SPT Propellant System

Size. µm	Particle Number
3	≈ 70
6-10	24
11-25	2
25-50	1
over 51	0

Pressure was indicated by a capacitance manometer that was calibrated to an accuracy of ± 0.25% at 36.25 PSIA, the nominal working pressure for the SPT-100. The propellant lines were leak-checked by pressurizing the lines, timing valve HV-1, and noting the pressure drop for several days. The leak rate was found to be less than 4x 10⁻⁴ sccm. It should be noted here that the pressure is dropped to the level required by the cathode and discharge chamber within the xenon flow control system (XFC) that came with the SPT-100 and is located directly behind it in the vacuum system. Therefore pressure in all propellant tubing is above atmospheric pressure up to the SPT XFC. Any xenon contamination should then be due to contaminants picked up from tubing walls, propellant system components, or the xenon itself. The purity of the xenon used by the SPT was tested from the xenon bottle itself. Purity data are shown in Table 2; the data show that the specifications (99.999%) were exceeded.

Table 2. Xenon Purity Tested from the Xenon Bottle

Impurity	Guarantee ppm	Actual ppm
Ar	1	<1
H	2	<2
Kr	5	<5
N ₂	2	<2
O ₂	0.5	<0.1
H ₂ O	0.5	<0.1
CO ₂	1	<1
THC	0.5	<0.5

A thermal mass flow meter was used to measure propellant flow rate. The flow meter was calibrated on both nitrogen and xenon by the manufacturer using a primary calibration standard, and at JPL using a bubblic volumeter. The calibration data indicate that the nitrogen calibration

performed at J 11, agrees with the primary standard calibration to within 1%, for all flow rates tested. The bubble volumeter data on xenon were curve fit and the curve fit was incorporated into the SPT data acquisition and control program,

A xenon recovery system is used to recover and store xenon consumed by the S11-100. The recovery system is used in the event of a cryopump failure or when 3000 liters of xenon have been consumed. A mechanical pump in the recovery system pumps the xenon out of the vacuum tank and into a holding tank chilled with liquid nitrogen; the vacuum tank is pumped by the recovery system pump to less than 0.4 torr pressure. Oil traps prevent recovery system pump oil from entering the vacuum tank.

A probe rake, consisting of 25 Faraday probes of diameter 2.3 cm each, mounted on a semicircular arc 2.4 m in diameter was used to examine the thruster exhaust plume. The probe buttons were biased to -23 volts when used to measure the plume shape. The probe rake was positioned such that the thruster is at the center of the semicircular arc; the axes of the rake were aligned with the plane formed by the outer insulator of the S11-100 such that the rake can be pivoted around a line normal to the thruster axis. This configuration enables complete hemispherical pictures of the exhaust plume to be obtained. When the probe rake is not in use, a motor rotates the rake to a position of approximately 90 degrees with respect to the thruster axis.

The SP1-100 is mounted to an inverted pendulum style thrust stand of the type developed at NASA LeRC; in this design, thrust is indicated by a linear voltage displacement transducer (JVIDT). The thrust stand is surrounded by a water-cooled housing to minimize temperature effects on the measured thrust. The thrust stand inclination is adjusted every 30 sec by computer to improve the accuracy of the thrust measurement over extended test times. Thrust stand calibrations are performed in-situ throughout the life test in the vacuum chamber using a set of weights deployed with a motor. Normally 40-80 calibrations are performed autonomously in order to obtain a large enough sampling for statistical analyses. Statistical analyses of the calibration data was also used to determine the thrust stand inclination. Repeatability of the calibrations were normally 0.6% or better.

The thruster is operated with a bread board power conditioning unit (PCU) developed by Space Systems/Loral. Preliminary data imply that the bread board PCU is approximately 93% efficient. The S11-100 (discharge current and magnetic field current are adjusted by supplying the appropriate voltage input signal to the PCU. The PCU output voltage is fixed at approximately 300 V. Propellant flow rate was controlled by the SPT-1 flow control unit which is part of the thruster; the mass flow rate was determined by the discharge current setting. The PCU was turned on and off by supplying the appropriate digital voltage pulse to the PCU. Once the engine parameters were adjusted and the PCU was turned on, the SP1-100 thruster was started and operated automatically by the bread board PCU. The PCU sequencing is described in Table 111.

Table 3. Power Conditioning Unit Sequencing

Time sec	Action
0	PCU start command received from computer
10	Cathode heater, capillary current, magnetic field current on
170	Cathode igniter voltage applied; cathode heater turns off.
171	SPT achieves 1.5 A discharge; run time clock started, begin on-phase
180	SPT achieves 4.5 A discharge
3180	S11-100 turned off by stop command issued by computer; begin off-phase
4380	PCU start command received from computer for next cycle

Stable-state thruster operation, start-up and shutdown sequencing are controlled by a PC based data acquisition system. This system also monitors the vacuum facility enabling unattended operation. A total of 56 channels that include thrust, xenon mass flow rate, anode voltage and current, floating voltage, magnet current, cathode heater current, thermo-throttle current, SPT inlet xenon pressure, tank pressure and various other facility components are monitored and recorded as a function of time. It takes 2 msec to scan each channel. All 56 channels are scanned 20 times, which required 2.4 sec. The data from the 20 scans are then averaged and the averaged values are displayed on a monitor screen. The data are recorded on the computer hard disc drive every 60 seconds, and printed every 120 seconds.

The computer is responsible for issuing the PCU start and stop commands. If certain engine or facility parameters exceed specifications, the computer sends the PCU stop command to the PCU, opens a relay between the PCU and its power source, closes the solenoid valve to stop xenon flow, and activates a telephone answering machine, (autodialer). The computer sends a change-of-state signal every 15 seconds to an electronic timer (heartbeat box); in the event of a computer failure, the timer activates a series of relays to turn off PCU power, xenon flow, and activates the autodialer.

The data acquisition program averages and stores PCU telemetry for discharge current, cathode heater current, and capillary current, and PCU output voltage for the discharge voltage. PCU telemetry for discharge voltage was compared to the discharge voltage measured at the vacuum

tank feedthrough; typically the voltage drop between the PCU and feedthrough was approximately 1.6 V. PCU telemetry for various SP1"-100 currents were calibrated to values obtained from calibrated current shunts. The discharge current calibration was determined using a voltmeter which averages the direct-current value of the discharge current shunt voltage drop over a period of four sec. ends. Oscillations in the discharge current were obtained with inductive probe placed on the discharge current cable close to the vacuum tank feedthrough. The discharge voltage ripple was measured at the vacuum tank feedthrough as well, using a combination inductive/plan effect probe. Cabling length between the feedthrough and SPT is approximately 6 m (Fig. 1). After cycle 663 of the cyclic life test the RMS value of the discharge current was measured using a true RMS voltmeter.

The thruster is photographed periodically through a window in the vacuum system to document the condition of the thruster. Insulator thicknesses are determined from photographs by measuring the ratio of insulator width to the length of the outer edge of the outer insulator or inner edge of the inner insulator.

PROCEDURE

The SP1"-100 was purged with nitrogen when the mechanical pumps were used to pump the vacuum tank from atmosphere to 50 mTorr ; subsequent purges are performed using rsc. arc. h-grade argon. During the fraction of the life test conducted to date both the pressure regulator and solenoid valve SV-1 failed; after replacing these components the propellant lines were purged with xenon or argon, then xenon was flowed through the pump-out line for 3-5 hours. The thruster was then started only if the vacuum tank pressure indicated by the calibrated ion gauge read below 2×10^{-7} Torr. Following a facility shutdown (cryopumps off) and after re-establishment of high vacuum the SP1"-100 was purged with xenon at 55 seem for 3 hours; no purge was used during a facility shutdown. As of this writing the SP1"-100 life test thruster has not been exposed to atmosphere since it was installed on June 22, 1993.

A cycle is defined as any time the thruster achieves a discharge current of $>1.5 \text{ A}$. The first 25 cycles of the life test were used to test the data acquisition and control program, the facility, and the probe rake; in these cycles the thruster was operated for varying time periods, from less than one minute to over 60 minutes, and at varying discharge currents.

The computer performed the task of starting and stopping the thruster, taking data, and monitoring the facility. Life test cycles are nominally 50 minutes on and 20 minutes off, with an additional three minutes for cathode pre-heating. Cyclic oscilloscope traces of current oscillations in the discharge current and a.c. ripple in the discharge voltage were obtained approximately every 10 cycles. Approximately every 100 hours the life test was stopped for a short period of time to photograph the thruster, measure flow meter zero drift, and to re-calibrate the thrust stand (T/S).

Approximately every 100 hours a probe scan was obtained using the probe rake.

RESULTS AND DISCUSSION

I. Test Summary

A brief summary of the life test is compiled in Table IV.

TABLE V. Life Test Summary.

Cycle	Cumulative Run Time Hrs	Comments
1	1	Observed plasma glow in unused cathode
9	4.1	Replaced pressure regulator
10	4.2	Performed thrust stand (T/S) calibration check
13	5.1	Installed solenoid valve downstream of regulator
18	6.8	Operated SPT at 3.96 A
19	7.1	Operated SPT at 3.46 A
20	7.4	Operated SPT at 2.40 A
21	7.6	Measured performance vs tank pressure
22-2s	8.1	System check-out
26		Life test started; eff. = 49%
27	8.9	Computer-commanded shutdown; flow rate exceeded minimum limit
93	63.1	Printer and software failure; thruster operated w/o sufficient xenon for up to 20 min
94-97	63.3	System check-out
98		Performed thrust stand (T/S) calibration check; life test resumed
150	107.5	T/S calibration check
265	203.5	T/S calibration check
395	312.0	Flow meter zero-shift check
415	328.7	T/S calibration check
467	370.4	Computer shutdown commanded when SPT xenon supply pressure exceeded upper limit
468	370.8	Applied 1 A of external magnetic field current
469	371.6	Applied 2 A of external magnetic field current
470	372.5	Applied 1.5 A of ext. magnetic field current to all subsequent cycles unless otherwise noted
555	443.4	Cryopump cold head and LN2 valve failure; replaced components. Performed T/S cal.
556		Restarted life test
560	446.8	Engine did not start; anode voltage not achieved

573	458.5	Flow meter zero-shift checked
608	487.8	Computer-commanded shut-down; printer error at end of cycle
614	492.0	Computer-commanded shut-down; printer error
616	493.7	Turned off externally-applied magnetic field
617	494.s	Magnetic field = 1.5 A
633	507.9	Magnetic field = 2 A
663	533.0	Magnetic field = 2 A; rms current measurement initiated
672	540.6	Magnetic field = 0 A
673	541.4	Magnetic field = 2 A
675	542.3	Computer-commanded shut-down; insufficient xenon feed pressure
676	543.3	Computer-commanded shut-down; printer error
677	543.8	Computer-commanded shut-down; printer error; replaced pressure regulator and valve, replaced xenon bottle
679	545.0	Software error caused loss of computer heartbeat signal; PCU power relay opened
749	604.4	Magnetic field = 2 A
755-757	609.4	Magnetic field = 0 A
758	611.1	Magnetic field = 1.5A
800	647.()	Efficiency = 44 %

A glow in the non-operating cathode was observed in cycle 1 and all subsequent cycles. The glow may be due to a propellant leak in the SPT XFC. This S1'1'-100" thruster utilizes a propellant system with no absolute flow shut-off to the unused cathode,¹⁶ a design feature present in newer SPT thrusters. The cathode glow occasionally flickers on engine start-up and periodically disappears completely for approximately 3 seconds before reappearing. The glow in the unused cathode is visible in a photograph (Fig. 4) of the S1'1'-100 in operation.

Early in the life test the pressure regulator and valve S V- 1 failed. Pressure was regulated adequately, but xenon leakage through the regulator and solenoid valve during the off-phase, resulted in excessive pressurization of the propellant system. This resulted in operation of the SPT at 2.63 - 2.76 x 10⁵ kPa during the first 100 seconds of thruster operation (nominal SPT input pressure = 2.51 x 10⁵ kPa). The regulator and valve were replaced and the replacement components failed as well. A new regulator and valve were installed after cycle 677.

The first 25 cycles were used for system testing and thruster performance testing. Starting with cycle 26 the SPT- 100 was cycled for 50 minutes on and 20 minutes off, with 3 minutes for cathode pre-heating.

in 39 of the 800 cycles accumulated to date, the thruster was operated for less than the usual 50 minutes for a variety of reasons. The first 25 cycles were used for system testing and thruster performance testing. Seven shutdowns were performed by the computer; most of those shutdowns are related to printer failures, one shutdown was performed by the timer when it failed to receive a change of state signal from the computer within the required 5 seconds; this failure occurred while an operator was in the process of downloading data from the hard drive onto floppy discs.

Two of the computer-commanded shutdowns were due to xenon leakage, through a faulty pressure regulator and solenoid valve during the off-phase. Typically two minutes were required before pressure returned to normal; during this two minutes only a small amount of xenon flow was registered by the flow meter. Although the thruster was receiving the correct flow rate, the low flow rate temporarily indicated by the flow meter was registered as a fault by the control program and shutdowns were initiated.

During cycle 93 a software error resulted in operation of the SPT thruster for approximately 30 minutes without sufficient xenon flow. Unfortunately no data for this cycle was printed or stored. The software error was corrected and tested during cycles 94-97. On cycle 560 the SPT thruster did not start. The data from the printout indicate that the failure was not due to the SPT but rather a DAC system (no start signal sent to the PCU) or a PCU error occurred.

A controlled facility shutdown was performed after cycle 555, due to imminent failure of one of the cryopumps. During the shutdown the vacuum tank pressure increased to 3800 kPa when xenon frozen onto cryopump cold surfaces vaporized. The xenon was recovered by the xenon recovery system 60 hours after the shutdown, when the vacuum tank was pumped by the recovery system pump to less than 53 Pa. The vacuum tank was pumped down to high vacuum approximately 84 hours after shutdown. Research-grade argon was flowed through the thruster when the mechanical pumps were used to pump the tank to under 7 Pa. Prior to restarting the SPT was purged on xenon for three hours at a flow rate of 5.5 mg/s.

Prior to cycle 470 no externally-applied magnetic field was used. By run hour 372, the peak-to-peak current oscillations had increased, from 2 S p-p to 8A p-p; after cycle 470 an auxiliary magnet current of 1.5 A was added to the nominal operating mode of the thruster in order to reduce discharge current oscillations to acceptable levels. By cycle 700 oscillation amplitudes increased significantly despite continued application of 1.5 A of auxiliary magnetic field current. Throughout cycles 470-800 different levels of auxiliary magnetic field current were tested to assess effects on thruster operation and performance.

2. Test Data for Cycles 26-800

Engine parameters such as efficiency, discharge current and voltage, etc., for cycles 26-800 are shown in Figs. 5(a-i). The data represent values for each of 765 cycles

(data from cycles 1-25, 63, 79, 93, 95, 467, 614, 675-677, 750 were ignored) that were calculated by averaging the data for the last 20 minutes of each cycle. These data were analyzed to determine cycle-to-cycle changes in thruster operating characteristics. Thrust was determined by subtracting the I.VDT voltage four minutes after the S115 was turned off from the I.VDT voltage obtained from the 20-minute average, and multiplying by the appropriate thrust stand calibration factor. Efficiency and specific impulse were calculated using the values for thrust, mass flow rate, and engine power, averaged for the last 20 minutes of the cycle.

Tank pressure and mass flow : Generally the shape of the curve of tank pressure vs cycle number does not correlate well with the flow rate curve plotted in fig. 5 (a); vacuum tank pressure indicated by the calibrated ion gauge, increased by approximately 9% between cycles 30 to 800, while engine mass flow increased only 2.7%. The pressure indicated by the uncalibrated ion gauge located on the wall of the vacuum tank (Fig. 1) did not change; Cycle-to-cycle oscillations in indicated tank pressure decreased after the defective cryopump cold head was replaced (cycle. 555).

Most of the increase in mass flow rate occurred between cycles 26-200; mass flow increased abruptly after cycle 470, when 1.5 A of magnetic field current was applied, then began to decrease following cycle 550. There is generally a good correlation between increasing flow rate and decreasing floating voltage, increasing discharge voltage, and increasing efficiency, except in cycles 1-200. From cycle to cycle, however, the variations in mass flow rate do not correlate well with cycle-to-cycle variations in discharge voltage or floating voltage.

Floating voltage: Floating voltage vs cycle number is plotted in Fig. 5 (b); floating voltage decreased by approximately two volts, or 9%, between cycles 30 and 800. Early in the life test cycle-to-cycle oscillations in floating voltage varied by 0.4 V p-p. The floating voltage decreased approximately 1 V after the software failure which occurred on cycle 93, but the basic characteristics of the floating voltage curve did not change. Beginning at approximately cycle 200 the cycle-to-cycle oscillations in floating voltage increased, approaching 2 V p-p by cycle 300. At cycle 469, where an auxiliary magnetic field current of 1.5 A was applied, floating voltage decreased approximately 3 V. At cycle 757, where there was no auxiliary magnetic field, the floating voltage was -19.3 V; at cycle 200 the floating voltage was -19.4 V.

The largest cycle-to-cycle variations (1-3 V) in the floating voltage are due to changes in the auxiliary magnetic field current; these oscillations occur between cycle 470-800. Smaller oscillations of approximately 1V or less are related to changes in thruster operating characteristics that will be discussed in the section of this paper concerning thruster efficiency and thruster operating modes; these oscillations correlate well with the discharge voltage and thruster efficiency.

Discharge voltage: Discharge voltage as a function of cycle number is plotted in Fig. 5 (c); discharge voltage decreased by approximately 3 V, or 1%, between cycles 30 and 800. The discharge voltage increased 0.5 V after the software failure which occurred on cycle 93, but like the floating voltage, the basic characteristics of the curve did not change. Beginning at approximately cycle 200 the cycle-to-cycle variations in discharge voltage increased, approaching 2 V by cycle 300, and the discharge voltage began to decrease. At cycle 469, where an auxiliary magnetic field current of 1.5 A was applied, the discharge voltage increased approximately 1 V, and cycle-to-cycle variations in discharge voltage decreased to less than 0.3 V. Discharge voltage continued to decline. At cycle 556, the first operating cycle following the cryopump repairs, discharge voltage increased 1.3 V; the engine was purged for 3 hours at a flow rate of 55 sccm prior to cycle 556, but it may be necessary to maintain a purge at all times when the cryopumps are not in operation. At cycle 757, where there was no auxiliary magnetic field, the discharge voltage was 296.5 V; at cycle 200 the discharge voltage was 299.5 V.

Following cycle 469, the largest cycle-to-cycle oscillations in the discharge voltage are associated with changes in the auxiliary magnetic field current. The smallest oscillations (approximately 0.5 V) are due in part to cyclical changes in thruster operating characteristics that correlate well with floating voltage and thruster efficiency. An example of how discharge voltage correlates with thruster efficiency from cycle-to-cycle is shown in Fig. 5 (j).

Discharge current: Discharge current vs cycle number is plotted in Fig. 5 (d). Discharge current was maintained at 4.5 A after cycle 20 by the CIOCC100P control system of the XFC. Discharge current varied by only ± 0.01 A throughout the test. Cycle-to-cycle oscillations in the discharge current generally do not track well with mass flow rate, floating voltage or discharge voltage.

Thrust, Efficiency, and Isp: Thrust data as a function of cycle number for all cycles are shown in Fig. 5 (e). Thrust was determined by the voltage difference between the thruster on and off phases of the (I.VDT); the I.VDT off-phase voltage, 4 minutes after thruster shutdown was used to calculate thrust. Although this method potentially increases the error in thrust measurement due to temperature drift, it decreases the error due to improper thrust stand inclination.

I.VDT data are shown in Fig. 5 (f). The large peaks located at cycle 755 and cycles 770-780 are due to uncontrolled thrust stand inclination. Small oscillations of 0.1 V p-p in the I.VDT off-phase voltage occurred every 24 hours, and are probably due to small movements of the I.VDT sensor as the vacuum tank heated up and cooled off. The only other major shifts in I.VDT off-phase voltage occurred between cycles 92-99 and cycles 555-556, where long periods of time occurred between cycles.

Thrust decreased 1 mN between cycles 30-467; thrust increased 2 mN at cycle 470, when auxiliary magnetic field current was applied to the thruster. Thrust decreased to

80.5 mN by cycle 800. Cycle-to-cycle variations in thrust correlate with variations in discharge voltage; an example is shown in Fig. 5 (g).

Engine efficiency vs cycle number is plotted in Fig. 5 (h). Error analyses indicate that overall thruster efficiency uncertainty is $\pm 4\%$ of the efficiency. The thrust measurement uncertainty in this analysis is $\pm 1.5\%$. Of the data shown in Fig. 5 (h), 36 data points exceed the uncertainty in the thrust measurement. 11 of these data are due to uncontrolled thrust stand inclination (cycles 755, 770-780); 5 are associated with application of an auxiliary magnetic field (cycles 616, 633, 673, 749).

Virtually all the remaining 20 cycles with efficiencies outside the uncertainty occur at cycle numbers which are located at peaks or troughs in Fig. 5 (b, c). The data indicate that measured variations in the thrust, discharge voltage, and floating voltage, and to a lesser extent mass flow rate (but not discharge current) may be indicative of true changes in thruster performance, and not to error in the thrust measurement. It should be pointed out here that in not every case, do peaks or troughs in discharge voltage result in large changes in efficiency. Additional investigations are required to identify the physics involved in the observed behavior of the SPT-100.

Selected thruster performance as a function of operating time is given in Fig. 5 (j). The different symbols plotted in this figure represent different values of auxiliary magnet current used to augment the normal electromagnet current (which is equal to the discharge current). The data were obtained as described above, except that thrust stand inclination was manually controlled and the LVDI off-phase voltage was obtained within 1-2 minutes after the thruster was shut off; in addition, the LVDI on-phase voltage was not averaged, but a single LVDI voltage was selected less than 60 seconds before thruster shutdown. Hence, the data indicate thruster performance shortly before thruster shutdown. The data indicate that thrust decreased approximately 5 mN between cycle 26 and cycle 800. Initially the efficiency was approximately 49%; after 350 hours of operating time the performance decreased to 46%.

The data in Fig. 5 (j) indicate that thrust efficiency increased when auxiliary electromagnet current was applied. After 300 hours of operation an auxiliary magnet current of 1.5 A was added to the nominal operating mode of the thruster in order to reduce the current oscillations back down to an acceptable level; efficiency immediately increased to 50%. However, by run hour 600 the magnetic field current of 1.5 A had no apparent effect on performance. Large cycle-to-cycle variations in thruster efficiency appear related to oscillations in the discharge current and discharge voltage.

Discharge Current Oscillations and Voltage Ripple: oscillations in discharge current and voltage are shown in Fig. 6 (a-f). A schematic diagram of the positions of the inductive/1 Hall effect probes is presented in Fig. 6 (g). The probes used to measure discharge current and voltage oscillations were positioned close to the vacuum tank

feedthrough. There is approximately 6 m of cable length between the tank feedthrough and the thrust stand.

Reduced current and voltage oscillation amplitudes are associated with improved thruster performance. Initially, discharge current oscillation amplitudes were generally less than 2 A p-p, and voltage ripple less than 2.5 V p-p (Fig. 6(a)). By cycle 28 current oscillation amplitudes up to 6 A p-p, and up to 5 V p-p ripple in the discharge voltage, although most peaks were below 2 A p-p. By cycle 200 most of the current oscillation peaks were approximately 6 A p-p; occasionally amplitudes exceeding 7-8 A p-p, for a direct current of 4.5 A, were observed.

Application of an auxiliary magnetic field current (performed at cycle 470) greatly reduced the magnitude of these oscillations, although the efficacy of the externally applied magnetic field current diminished relative to the effect obtained at cycle 470. The large variations in thruster performance observed between cycles 200-469, and to a lesser extent cycles 600-800, are related to the magnitude of the discharge current and voltage oscillations. Oscillations in current and voltage for cycle 800 are shown in Fig. 6 (f).

3. INDIVIDUAL CYCLE CHARACTERISTICS

Selected thruster parameters for cycle 26 (run hour 8.1) and cycle 800 (run hour 647) are plotted in Figs. 7 (a-f). Compared to cycle 800, parameters for cycle 26 such as thrust and discharge voltage are more consistent throughout the complete cycle. In cycle 26, such parameters as thrust, discharge voltage, and efficiency varied only slightly over the complete cycle. Significant and spontaneous changes in thruster operating characteristics some time after thruster start-up were observed beginning approximately with cycle 2.25. Increases in thrust were associated with reduced current and voltage oscillation amplitudes that were measured by the oscilloscope; rms values of discharge current generally decreased as well, from 5.2 A rms to as low as 4.6 A rms when discharge current oscillations were at a minimum.

When discharge current and voltage oscillation amplitudes are small (2 A p-p and 2 V p-p) compared to normal oscillation amplitudes (8 A p-p and 5 V p-p), the thruster is said to be operating in "quiescent mode". Quiescent mode operation has continued beyond cycle 800. Typically quiescent mode operation is observed to begin approximately 20 minutes after thruster start, and thrust remains at elevated levels until the cycle is completed. On the next cycle following thruster operation in quiescent mode, the thruster typically operates at reduced levels of performance until quiescent mode operation again occurs.

The transition to quiescent mode is shown in Fig. 8 (a-f) for data taken in cycle 330. Although mass flow increased 1.8% and discharge voltage increased 0.8%, indicated thruster efficiency increased 10%, due to a 6% increase in thrust which occurred more than 100 seconds after thruster startup. Discharge current did not change. On this particular cycle thrust began to decrease slightly just before the end of the cycle.

Oscilloscope traces of oscillations in discharge current and voltage for cycle 330 are shown in Figs. 8 (g-j). Discharge current oscillations of 6-9 A p-p and voltage oscillations of 5-10 V p-p were measured 24 minutes after engine start; engine efficiency was approximately 45%. Quiescent mode as indicated by the oscilloscope began approximately 25 minutes after engine start; 40 minutes after engine start current oscillation amplitudes dropped to 1-2 A p-p, with voltage oscillations of 2.5 V p-p; engine efficiency increased to 50%. Oscillation amplitudes began to increase shortly before the cycle ended. (oscillation amplitudes correlated with thrust and efficiency.)

4. Plume Characterization

A horizontal and a vertical slice of the exhaust plume obtained from the Faraday probe rake are shown in Fig. 9 (a), taken at cycle 757 (after approximately 600 hours of operation). Two horizontal slices taken at cycle 37 and cycle 757 are compared in Fig. 9 (b). There appears to be little gross change in the shape of the exhaust plume over this time period. However, the current density of the center probe along the thruster axis of cycle 757 may be 28% lower compared to the peak current density measured for cycle 37.

5. Performance as Function of Tank Pressure

The effect of vacuum tank pressure on engine performance was measured during cycle 21. Data are shown in Fig. 10. The data indicate that there was little effect of tank vacuum pressure on engine performance. However, when tank pressure exceeded approximately 5×10^{-5} torr in these tests, SPT discharge current and voltage oscillations increased substantially, SPT operation became somewhat more unstable and thruster performance decreased.

6. Insulator Erosion

Erosion of the discharge chamber insulator surfaces are documented photographically. Insulator thickness as a function of run hour is shown in Fig. 11. The data indicate that the outer insulator thickness has been reduced to 27% of its original 5.55 mm thickness; the inner insulator has been reduced in thickness to 72% of the original thickness. Preliminary results indicate an erosion rate that is approximately the same as reported in Ref. 17 for the outer insulator, and slightly less for the inner insulator. The data indicate that thruster efficiency correlates with insulator thickness, and that the erosion rate of the insulators is decreasing as the thruster ages. These data imply that the rate of decrease of thruster efficiency is itself decreasing.

A photograph of the SPT-100 after 600 hours of thruster-on-time is shown in Fig. 11 (a). By changing the lighting on the thruster the photograph in Fig. 11 (b) was obtained. This photograph clearly shows the "grooved" erosion pattern characteristic of long-term SPT operation. These grooves were noticeable after only 200 hours of thruster operation.

CONCLUSIONS

An endurance test of an SPT-100 is scheduled for 6,000 On/off cycles and 5,000 hours of operation at an input power of 1.35 kW. The endurance test was initiated July 1, 1993 and has accumulated 647 hours of operation and 800 on/off cycles as of this writing. The nominal cycle duration is 50 minutes on and 23 minutes off, including nearly three minutes of cathode preheat time. Thruster efficiency decreased, from 49% to 44% as the thruster aged; thruster efficiency increased when an auxiliary magnetic field was applied.

Variations in thruster performance from cycle to cycle appear related to variations in thruster operating characteristics such as floating potential and discharge voltage. Large variations in thruster performance are associated with oscillations in the discharge current and voltage. Significant variations in thruster performance were observed to occur within a single cycle; thruster operation frequently entered into a "quiescent mode" where current and voltage oscillations spontaneously decreased. Beam current density at the center of the plume decreased to 76% of the peak current density measured at the start of the life test. The outer insulator thickness decreased to 29% of the thickness measured at the start of the life test.

REFERENCES

1. Cary, E. C., Meyerand, R. G., Jr., and Salz, F., "Ion Acceleration in a gyro-dominated neutral plasma--theory and experiment", *Bull. Am. Phys. Soc.* 7 441 (1962).
2. Seikel, G. R., and Reshotko, E., "Hall-current ion accelerator", *Bull. Am. Phys. Soc.* 7 414 (1962).
3. Jones, G. S., Dotson, J., and Wilson, T., "Electrostatic acceleration of neutral plasmas -- momentum transfer through magnetic fields", *Proceedings of the 9th Symposium on Advanced Propulsion Concepts* (Gordon & Breach Science Publishers, Inc., New York, 1963) pp. 153-175.
4. Morozov, A. I. et al., "Plasma Accelerator with Closed Electron Drift and Extended Acceleration Zone", *Soviet Physics -- Technical Physics*, Vol. 17, No. 1, July 1972.
5. Bugrova, et al., "Physical Processes and Characteristics of Stationary Plasma Thrusters with Closed Electronics Drift", *IFPC-91-079*, October 1991.
6. Bober, A. et al., "State of Work on Electrical Thrusters in U.S.S.R.", *IFPC-91-003*, October 1991.
7. Artsimovich, L. A., "The Development of a Stationary Plasma Engine and its Test on Meteor Artificial Earth Satellite", *Space Explorations*, Vol. 12, No. 3, pp 451-468 (1974)

8. Arkhipov, B. A. et al., "SPT Electric Propulsion System for Spacecraft Orbit Maneuvering", Paper RGC-EP-92-07, 1st Russian-German Conference on Electric Propulsion, March 1992.
9. Brophy, J. R., "Stationary Plasma Thruster Evaluation in Russia, JPL Publication 92-4, March 15, 1992.
10. Brophy, J. R. et al., "Performance of the Stationary Plasma Thruster: SPT100", AI AA-92-31 55, 1992.
11. Patterson, M. J. et al. "Experimental Investigation of a Closed-Drift Thruster", AI AA-85-2060, 1985.
12. Cavney, I. H., Curran, F. M., and Brophy, J. R., "Russian Electric Space Propulsion Evaluated for Use on American Satellites", Paper RGC-EP-93-##, 2nd Russian-German Conference on Electric Propulsion, Moscow, Russia, July 1993.
13. Vladimir Kirin, personal communication, Moscow Aviation Institute, June 26, 1993.
14. Matsunami, N. et al., "Energy Dependence of the Yields of Ion-Induced Sputtering of Monatomic Solids", IPPJ-AM-32, September 1983.
15. Haag, T. W. and Curran, F. M., "Arcjet Starting Reliability: A Multistart Test on 1 Hydrogen/Nitrogen Mixtures", AIAA-87-1061, May 1987. (NASA TM-898867).
16. T. Randolph, personal communication, Space Systems/Loral, June 24, 1993.
17. Absalamov, S. K. et al., "Measurement of Plasma Parameters in the Stationary Plasma Thruster (SPT-100) Plume and its Effect on Spacecraft Components", AIAA-92-3156, July 1992.
18. Arkhipov, B. A. et al., "Anomalous erosion of an insulator under action of a stream of plasma", Phys. Plazmy 18 1241-1244 (Sept. 1992).

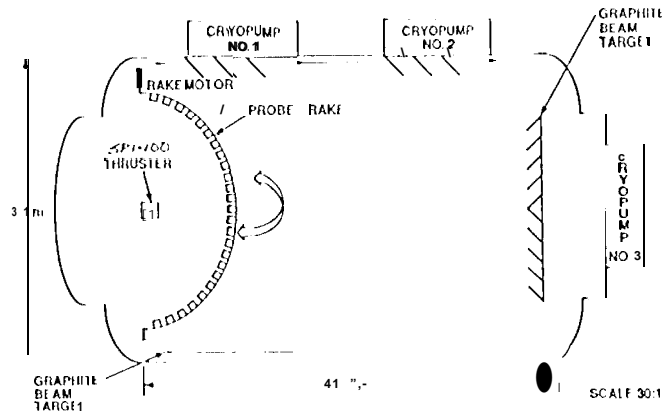


Fig. 1. SPT-1(X) cyclic endurance test facility.

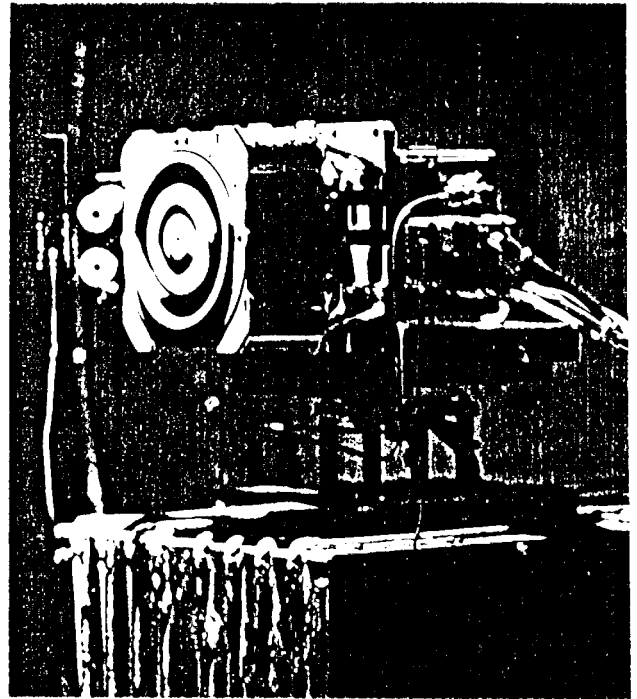


Fig. 2. SPT-100 mounted on a water-cooled thrust stand inside the vacuum chamber.

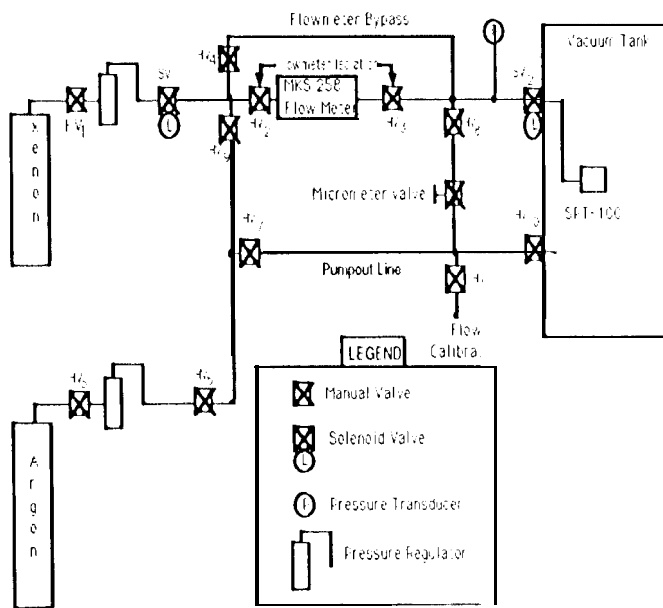


Fig. 3. Propellant system used to supply xenon to the SPT-100.

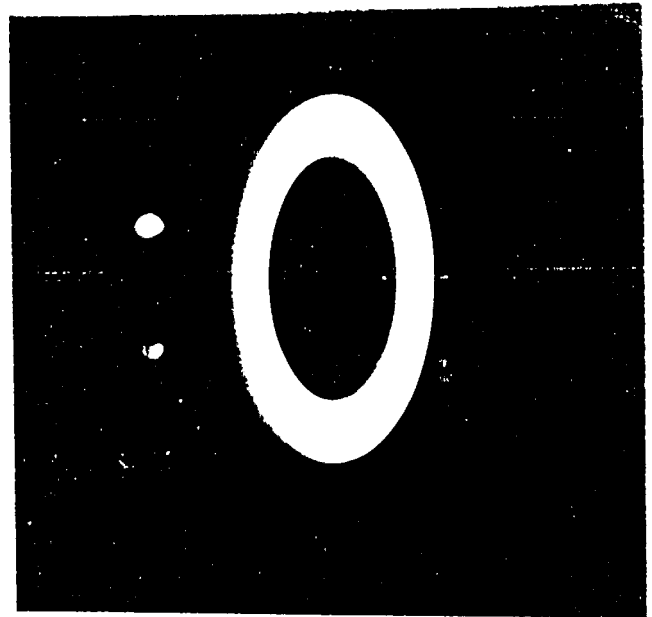


Fig. 4. Photograph of the SPT-100 in operation. Note the plasmaglow emanating from the unused (bottom) cathode.

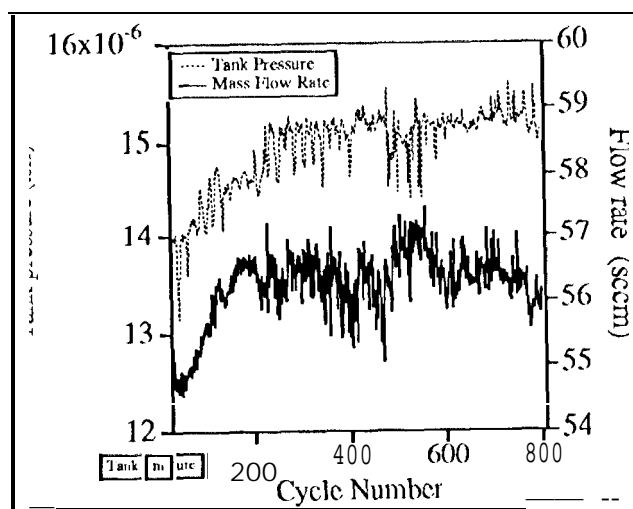
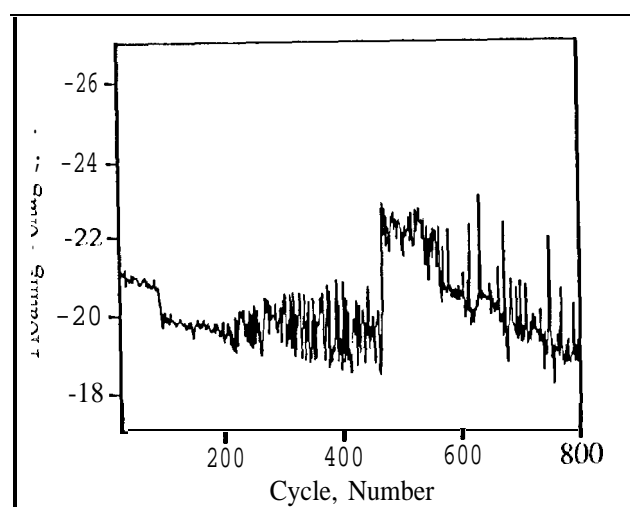


Fig. 5 (a). Tank pressure and mass flow rate vs cycle number.



Discharge voltage vs cycle number.

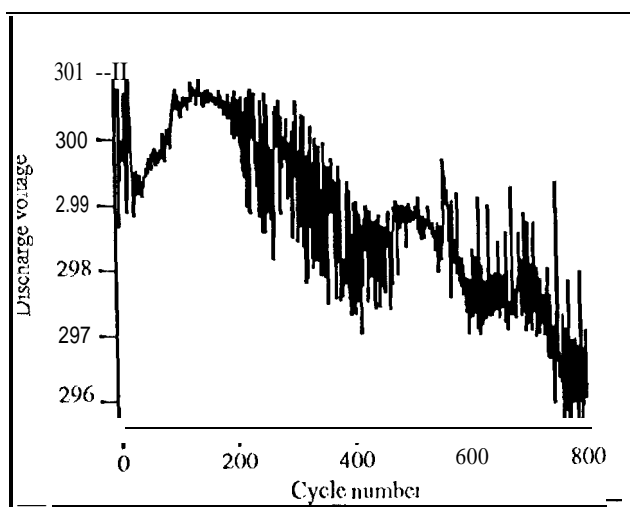


Fig. 5 (c). Discharge voltage vs cycle number.

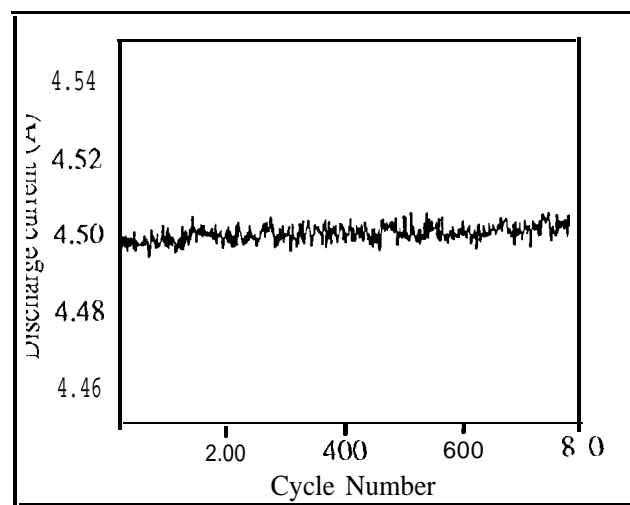


Fig. 5 (d). Discharge current vs cycle number.

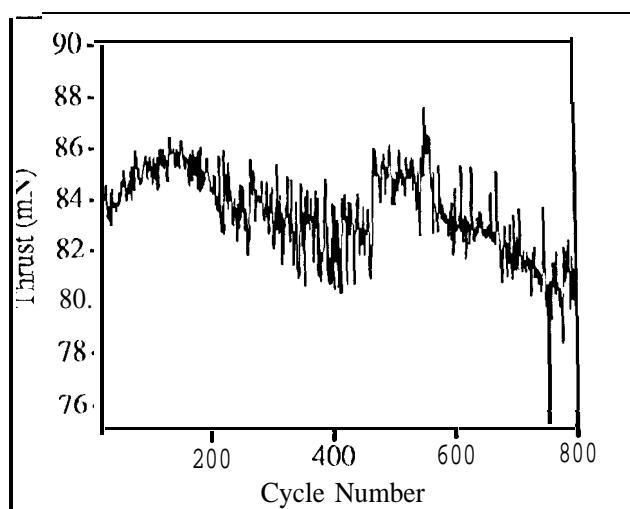


Fig. 5 (e). Engine thrust vs cycle number.

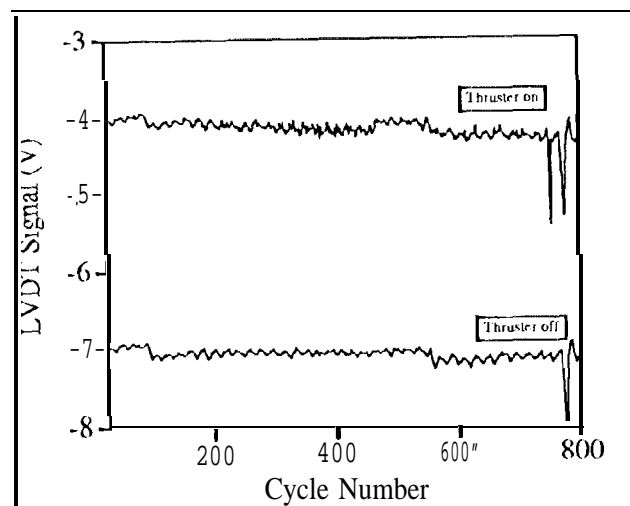


Fig. 5 (f). LVDT voltage vs cycle number.